J. Fluid Mech. (1989), *vol.* 206, *pp.* 155–170
Printed in Great Britain

Open channel flows with submerged obstructions

By FRÉDÉRIC DIAS[1] AND JEAN-MARC VANDEN-BROECK[2]

[1] Department of Mathematical Sciences, Worcester Polytechnic Institute, Worcester, MA 01609, USA

[2] Department of Mathematics and Center for the Mathematical Sciences, University of Wisconsin-Madison, Madison, WI 53705, USA

(Received 10 August 1988 and in revised form 1 March 1989)

Free-surface flows past a submerged triangular obstacle at the bottom of a channel are considered. The flow is assumed to be steady, two-dimensional and irrotational; the fluid is treated as inviscid and incompressible and gravity is taken into account. The problem is solved numerically by series truncation. It is shown that there are solutions for which the flow is subcritical upstream and supercritical downstream and other flows for which the flow is supercritical both upstream and downstream. The latter flows have limiting configurations with a stagnation point on the free surface with a 120° angle at it. It is found that solutions exist for triangular obstacles of arbitrary size. Local solutions are constructed to describe the flow near the apex when the height of the triangular obstacle is infinite.

1. Introduction

Free-surface flow past an obstacle at the bottom of a channel is considered. The fluid is assumed to be inviscid and incompressible and the flow to be steady and irrotational. Far upstream the flow is uniform with constant velocity $\tilde{U}$ and constant depth $\tilde{H}$ (see figure 1*a*). We define the upstream Froude number

$$\tilde{F} = \frac{\tilde{U}}{(g\tilde{H})^{\frac{1}{2}}}. \tag{1.1}$$

Here g denotes the acceleration due to gravity. The upstream flow is said to be subcritical when $\tilde{F} < 1$ and supercritical when $\tilde{F} > 1$.

Lamb (1945) calculated the flow past a submerged semi-elliptical obstacle by an approximate linear theory. He obtained solutions with a train of waves downstream for $\tilde{F} < 1$ and solutions without waves for $\tilde{F} > 1$. Recently Forbes & Schwartz (1982) and Forbes (1981) solved the corresponding exact problem numerically. They considered both semicircular and semi-elliptical obstacles. Their results confirm and extend Lamb's solutions.

In this paper we calculate the flow past a submerged triangular obstacle by a series truncation procedure. This technique has been used successfully by Brodetsky (1923), Birkhoff & Zarantonello (1957), Vanden-Broeck (1984), Vanden-Broeck & Keller (1987), and Dias, Keller & Vanden-Broeck (1988) to calculate nonlinear free-surface flows. Solutions with waves downstream are not considered in this paper. Therefore, we assume that the flow approaches a uniform stream with constant velocity U and constant depth H far downstream and we define the downstream Froude number F by

$$F = \frac{U}{(gH)^{\frac{1}{2}}}. \tag{1.2}$$

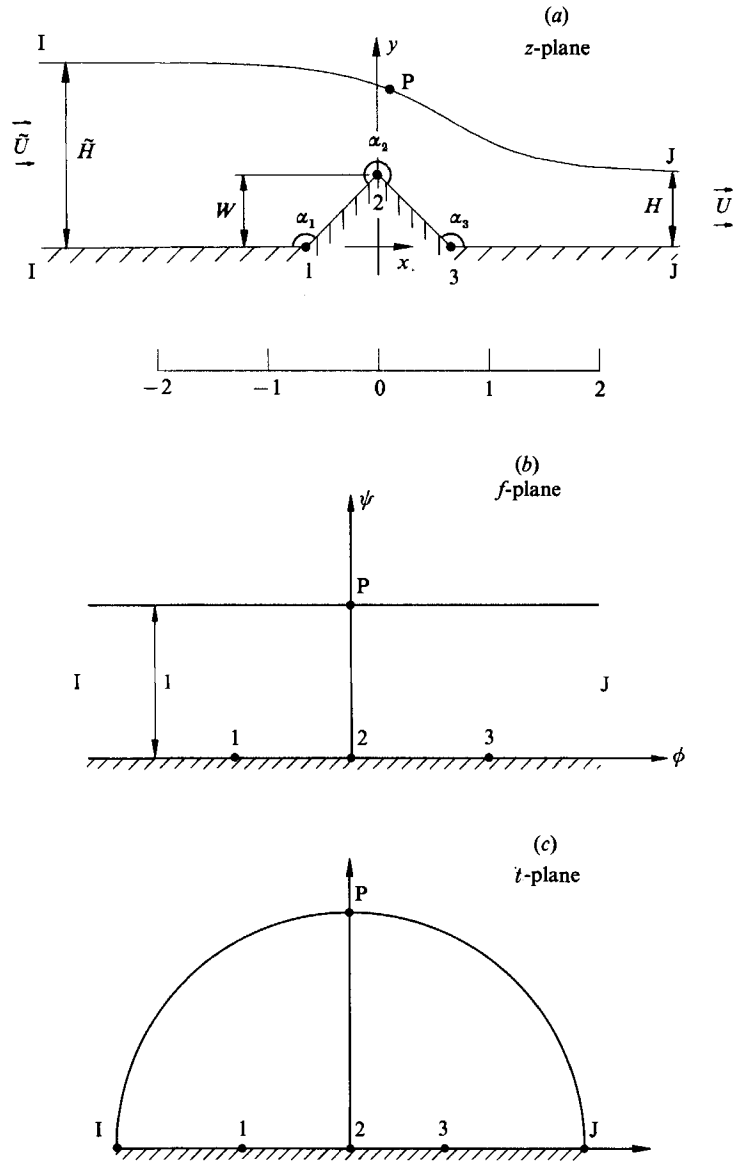

FIGURE 1. (*a*) Sketch of the flow and of the coordinates. Six special points are labelled on the boundary. The flow is uniform far upstream and downstream with velocities $\tilde{U}$ and U, and depths $\tilde{H}$ and H. The obstacle is a triangle of height W. The free-surface profile is a computed solution for $t_3 = 0.70$. The vertical scale is the same as the horizontal scale. The corresponding values of the Froude numbers are $F = 1.87$ and $\tilde{F} = 0.49$. (*b*) The complex potential plane. The images of the six points are shown. (*c*) The complex t-plane. The images of the six points are shown.

Our results show that there are solutions without waves for which the flow is subcritical upstream (i.e. $\tilde{F} < 1$) and supercritical downstream (i.e. $F > 1$). The flows far upstream and far downstream are conjugate flows (Benjamin 1966). Such flows were recently calculated by Forbes (1988) for a submerged semicircular obstacle. Our results for small triangles are qualitatively similar to those of Forbes. We show that there are solutions for triangles of arbitrary size. As the size of the triangle increases,

$\tilde{F} \to 0$ and $F \to \infty$. The corresponding limiting configuration near the apex of the triangle is a flow past an angle with one free surface which runs along the wall downstream (see figure 4). We calculate this limiting solution by using the numerical procedure derived by Vanden-Broeck & Keller (1986) to compute pouring flows.

We also calculate solutions that are supercritical both upstream and downstream. These solutions are characterized by $F = \tilde{F} > 1$. It is found that for a given triangle these supercritical solutions exist only for values of F greater than some particular value. Furthermore, for some values of F, there are two supercritical solutions. One is a perturbation of a uniform stream whereas the other is a perturbation of a solitary wave. These results are similar to those obtained by Vanden-Broeck (1987) for the flow past a semicircular obstacle. We show that for any given triangle there is a limiting configuration with a stagnation point on the free surface with a 120° angle at it (see figure 8). Furthermore we found that solutions exist for triangles of arbitrary size. As the size of the triangle increases the limiting flow near the apex of the triangle is a flow past an angle with one free surface running along the walls downstream and upstream (see figure 9). We calculate these flows for various angles.

The problem is formulated in §2, and the various solutions and limiting configurations are presented in §§3–6.

2. Formulation of the problem

We consider the steady irrotational flow of an incompressible inviscid fluid over a triangular obstacle (see figure 1*a*). A system of Cartesian coordinates is defined, with the x-axis along the bottom and the y-axis going through the apex of the triangle. Gravity acts in the negative y-direction. As $|x| \to \infty$, the flow approaches uniform streams with velocity $\tilde{U}$ and depth $\tilde{H}$ upstream, and velocity U and depth H downstream. The upstream Froude number $\tilde{F}$ and the downstream Froude number F are defined by (1.1) and (1.2) respectively. We define the discharge

$$Q = UH = \tilde{U}\tilde{H}. \tag{2.1}$$

The pressure is assumed to be constant on the free surface. By using the Bernoulli equation we write this condition as

$$\tfrac{1}{2}q^2 + gy = \text{constant on free surface}. \tag{2.2}$$

Here q denotes the magnitude of the velocity.

Following Binnie (1952) we use (2.1) and (2.2) to show that there are two different types of solutions. Evaluating (2.2) at $x = \pm\infty$ we obtain

$$\tfrac{1}{2}U^2 + gH = \tfrac{1}{2}\tilde{U}^2 + g\tilde{H}. \tag{2.3}$$

Combining (1.1), (1.2), (2.1) and (2.3) we find after some algebra

$$(\mu - 1)\left[\tfrac{1}{2}F^2(\mu + 1) - \frac{1}{\mu}\right] = 0. \tag{2.4}$$

Here

$$\mu = \frac{H}{\tilde{H}}. \tag{2.5}$$

Relation (2.4) shows that the two types of solutions correspond to

$$F^2 = \frac{2}{\mu^2 + \mu} \tag{2.6}$$

and

$$\mu = 1. \tag{2.7}$$

For the type (2.6) it can easily be shown that $\tilde{F} \leqslant 1, F \geqslant 1$ when $\mu \leqslant 1$ and that $\tilde{F} \geqslant 1, F \leqslant 1$ when $\mu \geqslant 1$. In this paper we assume $\mu \leqslant 1$ (see figure 1*a*). Therefore the flow is subcritical upstream and supercritical downstream. These solutions are calculated in §3. For the type (2.7) it follows from (2.1) and (2.5) that $U = \tilde{U}$, $H = \tilde{H}$ and $\tilde{F} = F$. These solutions are considered in §5.

We introduce dimensionless variables by taking $(Q^2/g)^{\frac{1}{3}}$ as the unit length and $(Qg)^{\frac{1}{3}}$ as the unit velocity. The dimensionless discharge is now equal to 1. We define the complex potential $f = \phi + \mathrm{i}\psi$ in terms of the potential ϕ and the stream function ψ. Since ϕ and ψ are conjugate solutions of Laplace's equation, f is an analytic function of $z = x + \mathrm{i}y$. The bottom of the channel and the triangle are parts of a streamline on which we require $\psi = 0$. The free surface is another streamline on which $\psi = 1$. In terms of the dimensionless variables, the condition (2.2) becomes

$$(\nabla\phi)^2 + 2y = \text{constant on } \psi = 1. \tag{2.8}$$

The flow problem can be reduced to a problem in complex analysis. The complex potential f maps the flow domain conformally onto an infinite strip of height 1, as is shown in figure 1(*b*). Without loss of generality, we chose $\phi = 0$ at the apex of the triangle (point 2). We map this infinite strip onto the upper half of the unit disk with I and J corresponding to the points -1 and 1, respectively (see figure 1*c*), so that the solid boundary goes onto the real diameter and the free surface onto the upper half-unit circle. The images of 1, 2 and 3 are $t_1, t_2 = 0$ and t_3, respectively. The map is given by

$$f = \frac{2}{\pi} \ln \frac{1+t}{1-t}. \tag{2.9}$$

The problem is now to find an analytic function $z(t)$ satisfying the boundary condition (2.8) and mapping the streamline $\psi = 0$ into the channel bottom and the obstacle. We proceed indirectly by introducing the hodograph variable

$$\xi(z) = \frac{\mathrm{d}f}{\mathrm{d}z}(z) = u - \mathrm{i}v. \tag{2.10}$$

The quantities u and v are the x- and y-components of velocity, respectively. Then the problem becomes that of finding ξ as an analytic function of t satisfying

$$|\xi|^2 + 2y = \text{constant on } |t| = 1 \tag{2.11}$$

and the kinematic boundary condition on the real diameter ($-1 \leqslant t \leqslant 1$).

3. Solutions with subcritical flow upstream and supercritical flow downstream

In this section we consider the solutions corresponding to (2.6). We assume that $\mu \leqslant 1$ so that the flow is subcritical upstream and supercritical downstream (see figure 1*a*).

Since there are angled corners at $t = t_1$, $t = 0$ and $t = t_3$, ξ must have singularities at these points. The appropriate singularities are

$$\xi \sim (t - t_1)^{1-\alpha_1/\pi} \quad \text{as} \quad t \to t_1, \tag{3.1}$$

$$\xi \sim t^{1-\alpha_2/\pi} \quad \text{as} \quad t \to 0, \tag{3.2}$$

$$\xi \sim (t - t_3)^{1-\alpha_3/\pi} \quad \text{as} \quad t \to t_3. \tag{3.3}$$

The angles α_1, α_2 and α_3 satisfy the relation $\alpha_1 + \alpha_2 + \alpha_3 = 3\pi$.

As $\phi \to +\infty$, the flow approaches a uniform supercritical stream. Therefore the asymptotic form of ξ as $\phi \to +\infty$ is obtained by linearizing the equations around a uniform stream and solving the resultant equations by separation of variables. This leads to

$$\xi \sim E + D\,\mathrm{e}^{-\lambda f} \quad \text{as} \quad \phi \to +\infty. \tag{3.4}$$

Here E and D are constants and λ is the smallest positive root of

$$F^2\lambda - \tan\lambda = 0. \tag{3.5}$$

In terms of the transformation (2.9) from f to t we rewrite (3.4) as

$$\xi \sim \xi(1) + A(1-t)^{2\lambda/\pi}. \tag{3.6}$$

We now define the function $\Omega(t)$ by the relation

$$\xi = \left(\frac{t-t_1}{1-t_1}\right)^{1-\alpha_1/\pi} t^{1-\alpha_2/\pi} \left(\frac{t-t_3}{1-t_3}\right)^{1-\alpha_3/\pi} \mathrm{e}^{\Omega(t)}. \tag{3.7}$$

The function $\Omega(t)$ has the following expansion:

$$\Omega(t) = A(1-t)^{2\lambda/\pi} + \sum_{n=0}^{\infty} a_n t^n. \tag{3.8}$$

The kinematic boundary conditions on the channel bottom and on the obstacle imply that the coefficients a_n are real. It can be checked that (3.7) in conjunction with (3.8) satisfies (3.1)–(3.4). The unknown real coefficients a_n and the constant A must be determined to satisfy the dynamic boundary condition (2.11) on the free surface.

Points on the free surface can be represented by $t = \mathrm{e}^{\mathrm{i}\sigma}\,(0 < \sigma < \pi)$. It is convenient to eliminate y from (2.11) by differentiating (2.11) with respect to σ. Using (2.9) and the identity

$$\frac{\partial x}{\partial \phi} + \mathrm{i}\frac{\partial y}{\partial \phi} = \xi^{-1} \tag{3.9}$$

we obtain

$$[u(\sigma)\,u_\sigma(\sigma) + v(\sigma)\,v_\sigma(\sigma)] - \frac{2}{\pi}\frac{v(\sigma)}{[u(\sigma)]^2 + [v(\sigma)]^2}\frac{1}{\sin\sigma} = 0. \tag{3.10}$$

We now set $t = \mathrm{e}^{\mathrm{i}\sigma}$ in (3.7) and (3.8) to get $\xi(\mathrm{e}^{\mathrm{i}\sigma})$ and substitute that expression in (3.10). We shall use the resulting equation to determine the coefficients a_n.

To do so we truncate the infinite series in (3.8) after $N-4$ terms. The calculations were restricted to isoceles triangles with a right angle at the apex. Thus we set $\alpha_1 = \frac{3}{4}\pi, \alpha_2 = \frac{3}{2}\pi, \alpha_3 = \frac{3}{4}\pi$. We fix the geometry of the triangle by specifying a value for t_3. We find the N unknowns t_1, λ, F, A and $\{a_n\}_{n=0}^{N-5}$ by collocation. Thus we introduce the $N-3$ mesh points

$$\sigma_M = \frac{\pi}{N-3}(M-\tfrac{1}{2}), \quad M = 1, \ldots, N-3$$

and satisfy (3.10) at these points. This leads to $N-3$ nonlinear algebraic equations. Relation (3.5) provides another equation. The last two equations are obtained by relating F to the velocity downstream and by rewriting (2.6) in terms of ξ. This leads to

$$F = |\xi(1)|^{\frac{3}{2}}, \tag{3.11}$$

$$F^2 = \frac{2|\xi(1)|^2}{|\xi(-1)|\,(|\xi(1)| + |\xi(-1)|)}. \tag{3.12}$$

This system of N nonlinear equations with N unknowns is solved by Newton's method. The ZSPOW package of the IMSL library was used for the computations.

Once this system is solved we can evaluate the complex velocity ξ by using (3.7). The upstream Froude number $\tilde{F}$ is given by the formula

$$\tilde{F} = |\xi(-1)|^{\frac{3}{2}}. \tag{3.13}$$

Next we calculate the profile of the free surface by integrating numerically (3.9) along the unit circle. This leads to

$$z(\sigma) = z(\tfrac{1}{2}\pi) - \frac{2}{\pi}\int_{\frac{1}{2}\pi}^{\sigma} \frac{1}{\xi(s)\sin s}\,\mathrm{d}s, \quad 0 < \sigma < \pi. \tag{3.14}$$

In order to evaluate $z(\frac{1}{2}\pi)$ we first calculate the height W of the triangle by integrating (3.9) from $t = 0$ to $t = t_3$:

$$W = \frac{1}{\sqrt{2}}\int_0^{t_3} \left(\frac{\mathrm{d}f}{\mathrm{d}t}\right)\frac{1}{\xi}\,\mathrm{d}t. \tag{3.15}$$

In (3.15) we used the fact that $\alpha_3 = \frac{3}{4}\pi$. The value of z at the point 2 is $z_2 = \mathrm{i}W$. We obtain $z(\frac{1}{2}\pi)$ by integrating (3.9) along the imaginary axis in the t-plane:

$$z(\tfrac{1}{2}\pi) = z_2 + \int_0^{i} \frac{\mathrm{d}f}{\mathrm{d}t}\frac{\mathrm{d}t}{\xi}. \tag{3.16}$$

The coefficients a_n were found to decrease rapidly. For example, for $W = 0.34$, $|a_1| \sim 2\times10^{-2}$, $|a_2| \sim 3\times10^{-3}$, $|a_8| \sim 10^{-4}$, $|a_{25}| \sim 10^{-6}$. Most of the calculations were performed with $N = 40$. However, for large triangles the coefficients a_n decrease less rapidly and N was increased to 135. For $W = 1.1$, $|a_1| \sim 10^{-1}$, $|a_2| \sim 3\times10^{-2}$, $|a_8| \sim 10^{-2}$ and $|a_{110}| \sim 10^{-6}$.

Typical profiles are shown in figures 1 (a) and 2. These results show that the size of the triangle increases as t_3 varies from 0 to 1. As $t_3 \to 0$, the triangle vanishes and the flow reduces to a uniform stream characterized by $F = \tilde{F} = 1$. As t_3 approaches 1, the triangle becomes infinite. The corresponding limiting flow configuration is calculated in the next section.

In figure 3 we present values of the height W of the triangle, versus the Froude number F. It shows that the flows considered in this section bifurcate from the uniform horizontal flow at the critical value $F = 1$ of the Froude number. As the triangle becomes larger, the Froude number increases and in the limit as $W \to \infty$, $F \to \infty$ and $\tilde{F} \to 0$.

4. Limiting flow configuration

In the last section we have shown that there is a one-parameter family of solutions for which the flow is subcritical upstream and supercritical downstream. The parameter can be chosen as the size of the triangle. As the size of the triangle increases, the flow near the apex of the triangle becomes similar to the flow over a wedge (see figure 4). We shall calculate this limiting flow configuration by using the numerical procedure developed by Vanden-Broeck & Keller (1986) to compute pouring flows.

The upstream side of the wedge, I2, slopes at an angle β from the horizontal. The t-plane and the f-plane are the same as before with point 1 coinciding with I and point 3 coinciding with J. As $x \to +\infty$, the flow approaches the thin wall jet flow of Keller

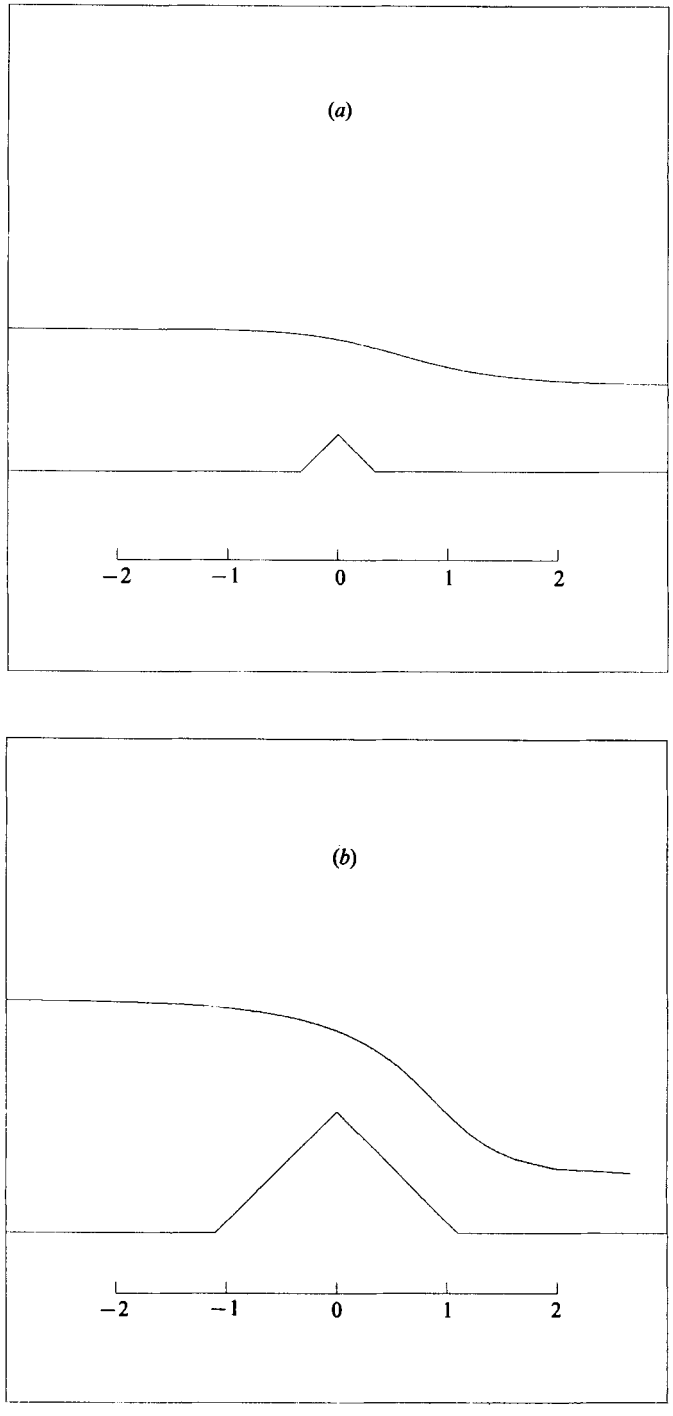

FIGURE 2. Same as figure 1(*a*) with (*a*) $t_3 = 0.40$, $F = 1.43$, $\tilde{F} = 0.68$; (*b*) $t_3 = 0.94$, $F = 2.49$, $\tilde{F} = 0.32$.

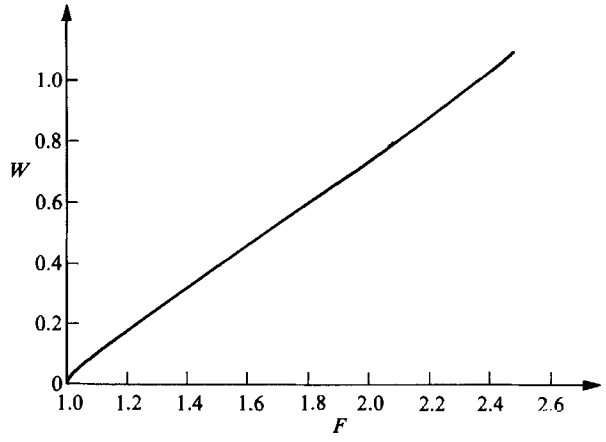

FIGURE 3. Values of the height W of the triangle versus the Froude number F.

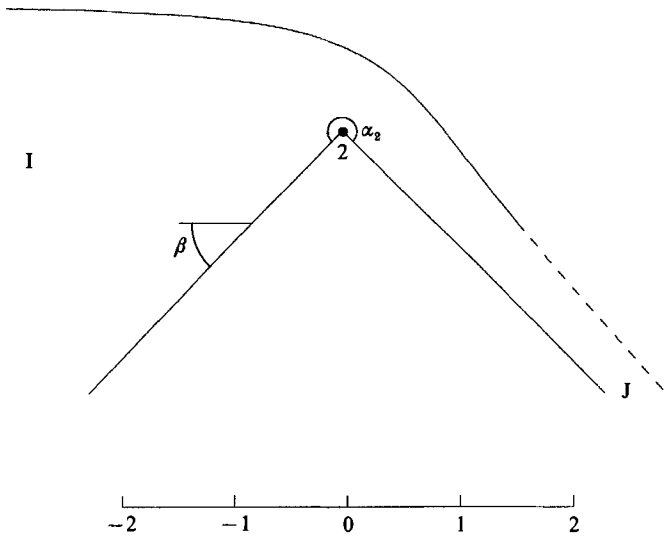

FIGURE 4. Free-surface flow over a wedge. It was calculated for $\beta = \frac{1}{4}\pi$ and $\alpha_2 = \frac{3}{2}\pi$. The broken line corresponds to the asymptotic solution (4.5). The vertical scale is the same as the horizontal scale.

& Geer (1973). The singularity at point 2 is still given by (3.2). But the singularities at I and J are now of the form

$$\xi \sim (1+t)^{2\beta/\pi} \quad \text{as} \quad t \to -1, \tag{4.1}$$

$$\xi \sim [-\ln(1-t)]^{\frac{1}{3}} \quad \text{as} \quad t \to 1. \tag{4.2}$$

Equation (4.1) represents a source-type singularity and (4.2) a jet-type singularity. Equation (3.7) is now replaced by

$$\xi = e^{i(\alpha_2-\beta-\pi)}(1+t)^{2\beta/\pi}t^{1-\alpha_2/\pi}[-\ln c(1-t)]^{\frac{1}{3}}\exp\left(\sum_{n=0}^{\infty} a_n t^n\right). \tag{4.3}$$

Here c is a constant. We assume that $0 < c < 0.5$ so that $[-\ln c(1-t)]^{\frac{1}{3}}$ is real for $-1 < t < +1$. We chose $c = 0.2$. We checked that the computed values of ξ evaluated

from (4.3) do not depend on the value of c chosen. However, different values of the coefficients a_n are obtained for different values of c. Vanden-Broeck & Keller (1986) studied a similar flow with $\alpha_2 = 2\pi$. Equation (4.3) reduces to their equation (27) after replacing α_2 by 2π and rotating the coordinate system by $-\frac{1}{2}\pi$.

The coefficients a_n are determined by using the collocation procedure described in §3. For given values of α_2 and β, the infinite series in (4.3) is truncated after N terms. N equations for the unknowns $a_0, \ldots, a_{N-1}$, are obtained by requiring that Bernoulli's equation be satisfied at N collocation points. This system of equations is solved by Newton's method.

The profile of the free surface for $\alpha_2 = \frac{3}{2}\pi$ and $\beta = \frac{1}{4}\pi$ is shown in figure 4. As $x \to +\infty$, the solution is described by the thin-jet theory (Keller & Geer 1973). If δ denotes the thickness of the jet, the velocity approaches the inverse of δ. We define coordinates x and y with the origin at the apex of the wedge. Since $\delta = -\sin(\alpha_2-\beta)\,x + \cos(\alpha_2-\beta)\,y$, we have

$$-\sin(\alpha_2-\beta)\,x + \cos(\alpha_2-\beta)\,y \sim |\xi|^{-1}. \tag{4.4}$$

Combining (4.4) with Bernoulli's equation (2.11) we obtain the equation for the free surface of the jet:

$$x \sim -y\cot(\alpha_2-\beta) - \frac{1}{\sin(\alpha_2-\beta)}\,(\text{constant} - 2y)^{-\frac{1}{2}}. \tag{4.5}$$

The relation (4.5) is represented by the broken curve in figure 4. The constant in (4.5) is obtained from the numerical results. It is interesting to compare figures 2(*b*) and 4, and to see that the solution for a large triangle is close to the limiting configuration, at least until the jet feels the bottom downstream.

5. Solution with supercritical flows both upstream and downstream

We now consider solutions corresponding to (2.7). As explained in §2, these solutions are characterized by $U = \tilde{U}$, $H = \tilde{H}$ and $F = \tilde{F}$ (see figure 5). We shall construct branches of solutions for which the flow is supercritical both upstream and downstream, i.e. $F = \tilde{F} > 1$.

Since the analysis is restricted to isoceles triangles, the problem is symmetric with respect to the y-axis. The singularities along the obstacle are still described by (3.1)–(3.3). The t-plane and the f-plane remain unchanged. But now the condition that the flow approaches a uniform stream exponentially is prescribed both downstream and upstream so that

$$\xi \sim E + D\,\mathrm{e}^{\mp\lambda f} \quad \text{as} \quad \phi \to \pm\infty. \tag{5.1}$$

Here λ is the smallest positive root of (3.5).

For $F = \infty$, the velocity is constant on the free surface, $\lambda = 0$ and the problem has an exact solution, namely

$$\xi = \xi(1)\left(\frac{t-t_1}{1-tt_1}\right)^{1-\alpha_1/\pi} t^{1-\alpha_2/\pi}\left(\frac{t-t_3}{1-tt_3}\right)^{1-\alpha_3/\pi}. \tag{5.2}$$

For $F \neq \infty$, we write

$$\xi = \left(\frac{t-t_1}{1-tt_1}\right)^{1-\alpha_1/\pi} t^{1-\alpha_2/\pi}\left(\frac{t-t_3}{1-tt_3}\right)^{1-\alpha_3/\pi} \mathrm{e}^{\Omega(t)}. \tag{5.3}$$

Here $\Omega(t)$ has the expansion

$$\Omega(t) = B(1-t^2)^{2\lambda/\pi} + \sum_{n=0}^{\infty} b_n t^{2n}. \tag{5.4}$$

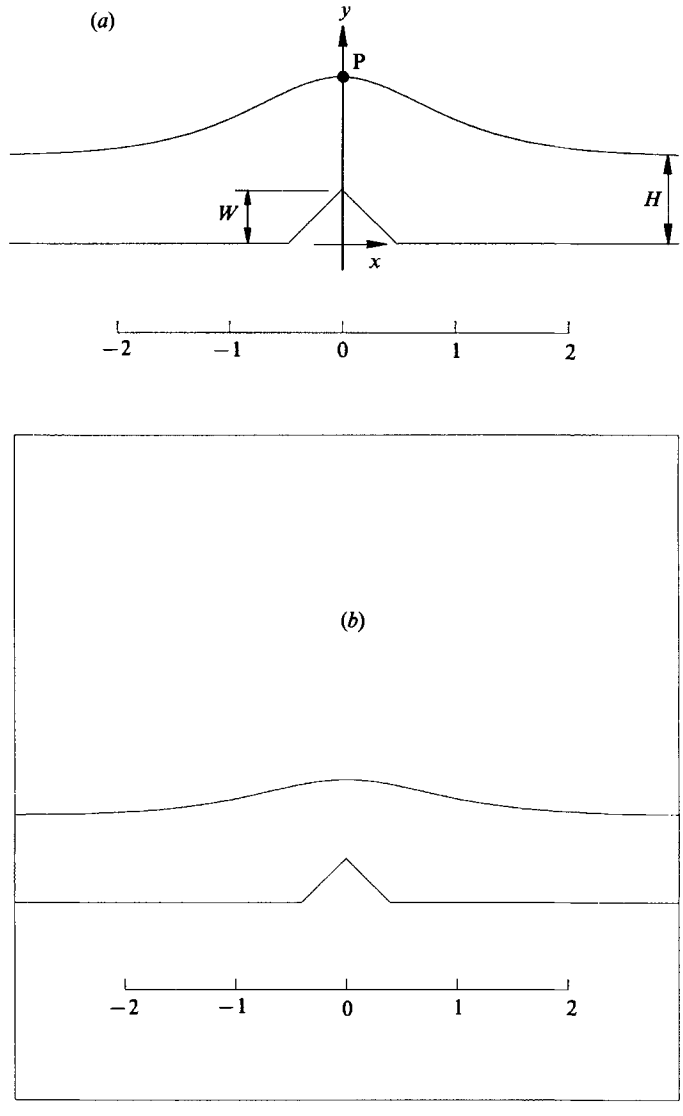

FIGURE 5. Computed solution with supercritical flows both upstream and downstream, for $t_3 = 0.5$ and (a) $F = 1.47$; (b) $F = 1.43$. The vertical scale is the same as the horizontal scale.

Since the flow is symmetric with respect to the y-axis, only even powers of t are used in (5.4). Furthermore, $t_1 = -t_3$ and $\alpha_1 = \alpha_3$.

The solutions described in this section depend on one more parameter than those studied in §3. Therefore we specify not only the channel and obstacle geometries but also the Froude number. Then we solve for λ and the coefficients in (5.4). We truncate the infinite series in (5.4) after $N-2$ terms, and solve for the N unknowns: $\lambda, A, b_0, b_1, \ldots, b_{N-3}$. $N-2$ equations are obtained by defining $N-2$ collocation points equally spaced on the portion IP of the unit circle in the t-plane (including the point P of maximum elevation). An extra equation is given by (3.5). The last equation relating F and the velocity at infinity is given by (3.11). The rest of the computations follows closely the calculations of §3. Typical solutions are shown in figure 5.

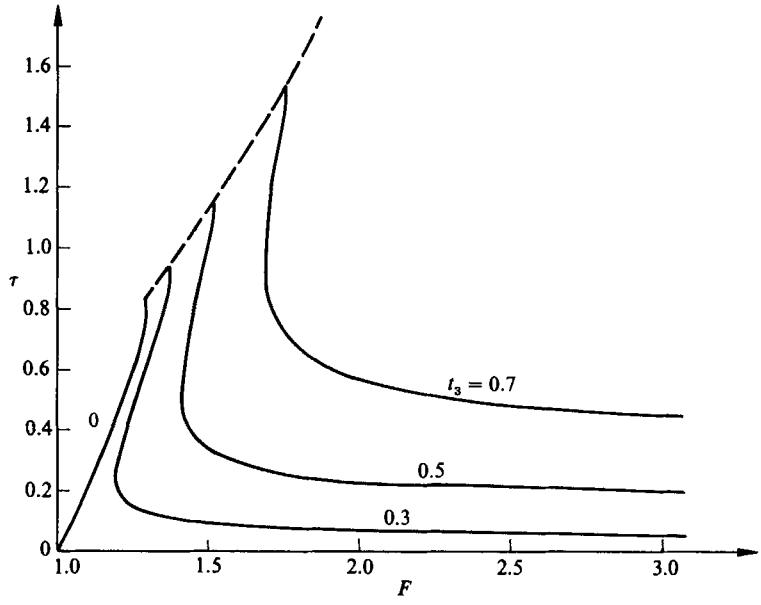

FIGURE 6. Numerical values of the maximum elevation τ of the free surface versus the Froude number F, for various values of t_3. The curve for $t_3 = 0{,}0$ corresponds to solitary waves. The broken curve corresponds to solutions with a stagnation point on the free surface (see (5.6)).

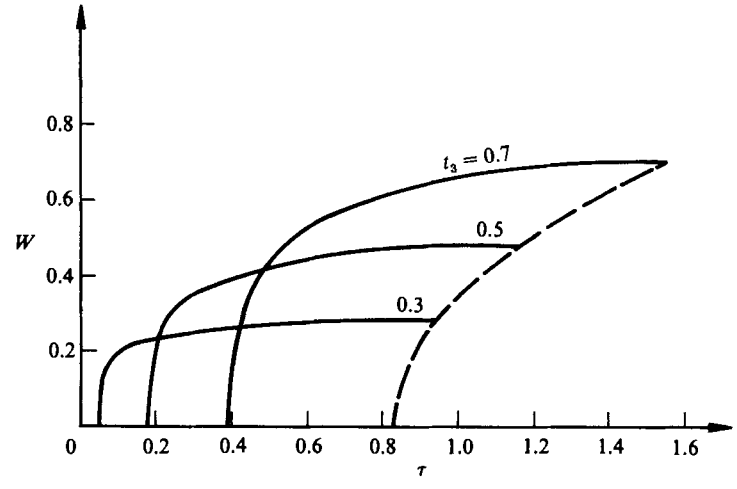

FIGURE 7. Values of the height W of the triangle versus the maximum elevation τ of the free surface, for various values of t_3. The broken curve corresponds to solutions with a stagnation point on the free surface.

A quantity of physical interest is the maximum elevation $y(\frac{1}{2}\pi)$ of the free surface at $x = 0$. It can be represented by the dimensionless parameter

$$\tau = \frac{y(\frac{1}{2}\pi)}{H} - 1. \tag{5.5}$$

τ is the maximum deviation of the free surface from its level at infinity divided by the water depth at infinity. In figure 6, we present numerical values of τ versus F for various values of t_3. The corresponding values of the height W of the triangle are shown in figure 7. As τ increases, the Froude number first decreases to a minimum

value $F^*(t_3)$ and then increases. Consequently, for a given t_3, there is no solution when $F < F^*$. On the other hand, for some values of F, there are two different solutions.

The results shown in figure 6 are similar to those obtained by Vanden-Broeck (1987) for the flow past a submerged semicircular obstacle. Following his analysis we consider the particular case $t_3 = 0$ (i.e. no obstacle). A uniform stream is then a trivial solution for any value of F. This corresponds to the F-axis in figure 6. Another branch of solutions for $t_3 = 0$ corresponds to solitary waves of arbitrary amplitude. This branch bifurcates from the uniform stream at $F = 1$ and is also shown in figure 6. For $t_3 \neq 0$ we denote by $\tau^*(t_3)$ the value of τ corresponding to $F^*(t_3)$. Then the solutions for $\tau < \tau^*$ can be viewed as perturbation of a uniform flow while the solutions for $\tau > \tau^*$ can be viewed as a perturbation of a solitary wave.

For a given t_3, there is a maximum value of τ, say $\tau_{\max}(t_3)$, above which no solutions exist. $\tau_{\max}$ corresponds to profiles with a stagnation point at P with an angle of 120° at it. When $t_3 = 0$, these solutions reduce to the well-known highest solitary wave. $\tau_{\max}$ can be expressed in terms of F by using Bernoulli's equation

$$\tau_{\max} = \tfrac{1}{2}F^2. \tag{5.6}$$

The curve corresponding to (5.6) is the broken curve in figure 6.

Both profiles shown in figure 5 correspond to $t_3 = 0.5$. In figure 5(b), the flow is a perturbation of a uniform flow and $W = 0.40, F = 1.43$. In figure 5(a), the flow is a perturbation of a solitary wave and $W = 0.48, F = 1.47$.

In order to compute the limiting configurations with a stagnation point at P, we modify the expansion (5.3) by including the term $[\frac{1}{2}(1+t^2)]^{\frac{1}{3}}$ to describe the singularity associated with the 120° angle. Thus we write

$$\xi = [\tfrac{1}{2}(1+t^2)]^{\frac{1}{3}}\left(\frac{t-t_1}{1-tt_1}\right)^{1-\alpha_1/\pi} t^{1-\alpha_2/\pi}\left(\frac{t-t_3}{1-tt_3}\right)^{1-\alpha_3/\pi} e^{\Omega(t)} \tag{5.7}$$

and we proceed as before. For $t_3 = 0$ the formula (5.7) reduces to the expression used by Hunter & Vanden-Broeck (1983) to compute the highest solitary wave. Figure 8 shows a limiting configuration with a 120° angle for $W = 0.48$ and $F = 1.52$.

The expansion (5.3) was found to be inadequate to compute solutions near the limiting configuration because an increasing number of terms was required as the 120° angle is approached. Therefore we used a different representation for ξ, namely

$$\xi = [\tfrac{1}{2}(2-\rho+\rho t^2)]^{\frac{1}{3}}\left(\frac{t-t_1}{1-tt_1}\right)^{1-\alpha_1/\pi} t^{1-\alpha_2/\pi}\left(\frac{t-t_3}{1-tt_3}\right)^{1-\alpha_3/\pi} e^{\Omega(t)}. \tag{5.8}$$

This type of expansion was first proposed by Havelock (1919). It has been used successfully by Vanden-Broeck (1986) to compute steep gravity waves. The parameter ρ in (5.8) is found as part of the solution. For ρ small the expansion (5.8) reduces to the expansion (5.3). Furthermore, for $\rho = 1$, (5.8) becomes (5.7). Therefore (5.8) combines the characteristics of the expansions (5.3) and (5.7). It was found to give very accurate results for all values of t_3.

6. Additional limiting flow configurations

As the size of the triangle increases, the solutions of §5 approach limiting configurations with a free surface following along the walls of a wedge (see figure 9). We shall extend the procedure of the previous sections to calculate these limiting flow configurations.

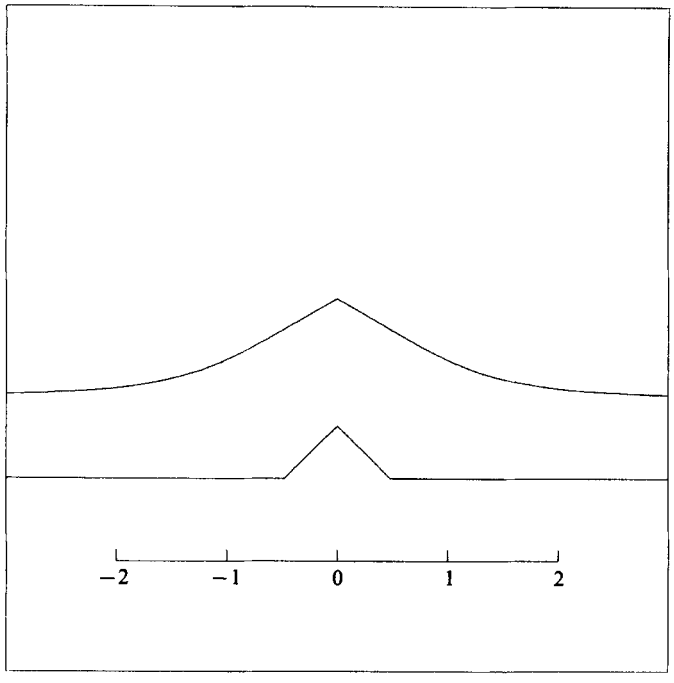

FIGURE 8. Limiting configuration for $t_3 = 0.5$ and $F = 1.52$. The height of the triangle is $W = 0.48$. There is a stagnation point on the free surface with a 120° angle at it. The vertical scale is the same as the horizontal scale.

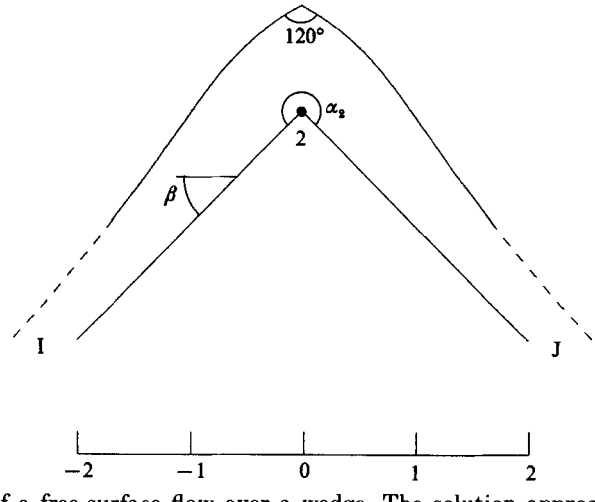

FIGURE 9. Sketch of a free-surface flow over a wedge. The solution approaches a thin jet both upstream and downstream. The broken curve corresponds to the asymptotic solution (4.5). The free surface is a computed solution with a stagnation point with a 120° angle at it, for $\beta = \frac{1}{4}\pi$ and $\alpha_2 = \frac{3}{2}\pi$. The vertical scale is the same as the horizontal scale.

We denote by β the angle between the wall I2 and the horizontal (see figure 9). The symmetry of the problem implies that $\alpha_2 = \pi + 2\beta$. As $|x| \to \infty$, the flow approaches the thin jet solution described in §4. The singularity at the point 2 is given by (3.2). Therefore we write

$$\xi = e^{i\beta} t^{1-\alpha_2/\pi} [-\ln c(1-t^2)]^{\frac{1}{3}} \exp\left(\sum_{n=0}^{\infty} b_n t^{2n} \right). \tag{6.1}$$

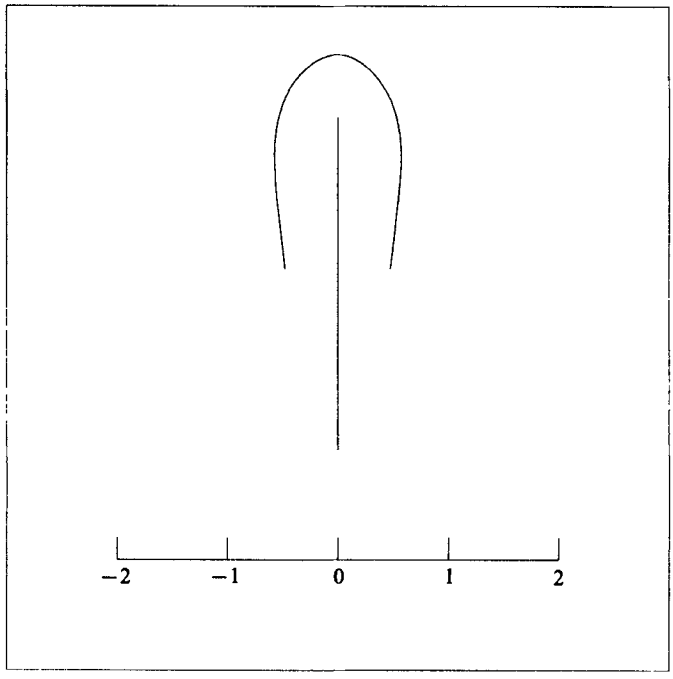

FIGURE 10. Free surface-flow past a semi-infinite vertical wall. The velocity at the highest point of the free surface is $\xi(i) = 0.5$. As $y \to -\infty$, the solution approaches thin jets on either sides of the wall. The vertical scale is the same as the horizontal scale.

We choose $c = 0.2$ and determine the coefficients b_n by the numerical procedure described in the previous sections. We note that we specify two parameters, β and the velocity $\xi(i)$ at the highest point on the free surface, in order to obtain a unique solution.

We consider first solutions with $\beta = \frac{1}{2}\pi$. Then the wedge reduces to a semi-infinite vertical wall. A typical profile for $\xi(i) = 0.5$ is shown in figure 10. In figure 11, we present numerical values of $\xi(i)$ versus the distance L between the highest point on the free surface and the apex of the wedge. As $\xi(i) \to \infty, L \to 0$ and the solution approaches the exact free-streamline solution:

$$\xi = \xi(i)\, e^{i\beta} t^{1-\alpha_1/\pi}. \tag{6.2}$$

Solution (6.2) was first derived by Keller (1957).

Integrating (6.2) we find after some algebra

$$\xi(i) = \left(\frac{2}{\pi} \ln 2\right) \frac{1}{L}. \tag{6.3}$$

Relation (6.3) is represented by the broken line in figure 11. It shows that our numerical results are in good agreement with the asymptotic formula (6.3) as $L \to 0$. Solutions were found to exist for all values of $\xi(i) \geqslant 0$. For $\xi(i) = 0$, there is a stagnation point on the free surface with a 120° angle at it. The corresponding profile is shown in figure 12. This solution was obtained by including the factor $(1+t^2)^{\frac{1}{3}}$ in the expansion (6.1) to describe the singularity associated with the 120° angle and by following the procedure outlined at the end of §5. The value of L corresponding to the profile of figure 12 is indicated by a cross in figure 11.

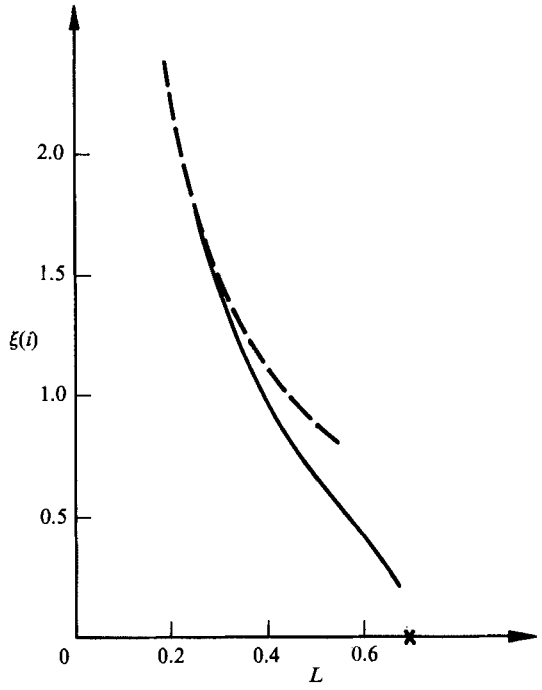

FIGURE 11. Numerical values of the velocity $\xi(i)$ at the highest point of the free surface versus the distance L between this point and the apex of the wedge, for $\beta = \frac{1}{2}\pi$ and $\alpha_2 = 2\pi$. The broken curve corresponds to the asymptotic formula (6.3) and the cross to the limiting configuration with a stagnation point.

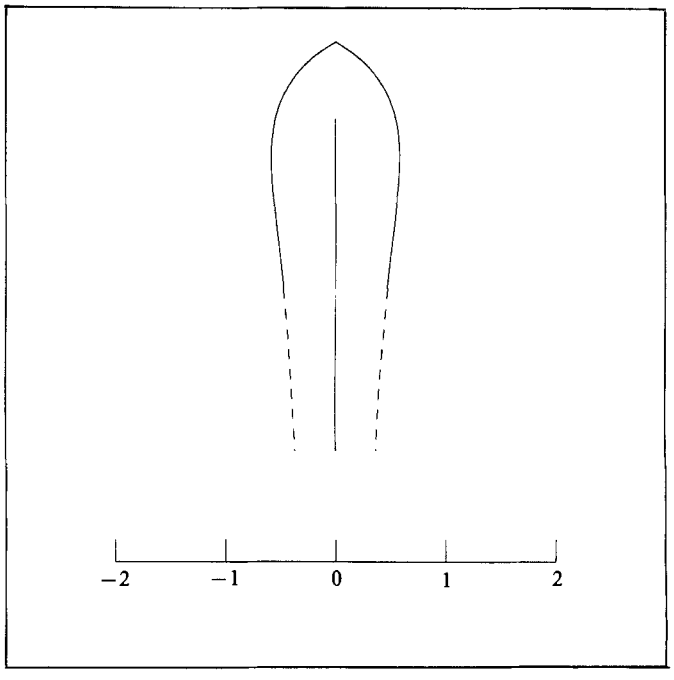

FIGURE 12. Same as figure 9 with $\beta = \frac{1}{2}\pi$ and $\alpha_2 = 2\pi$.

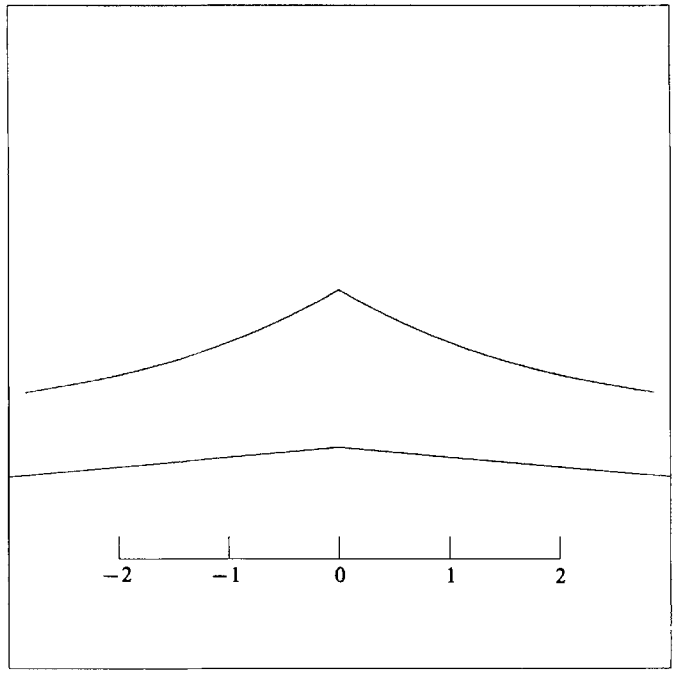

FIGURE 13. Same as figure 9 with $\beta = 5°$ and $\alpha_2 = 350°$.

Solutions with $\xi(i) = 0$ (i.e. with a stagnation point on the free surface) were obtained for various values of β. In figures 9 and 13 we present the solution for $\beta = 45°$ and $\beta = 5°$. As $\beta \to 0$, the flow approaches the highest solitary wave.

This work was supported by the National Science Foundation. Numerical computations were partly performed on a Cray at the San Diego supercomputer centre.

REFERENCES

BENJAMIN, T. B. 1966 *J. Fluid Mech.* **25**, 241.
BINNIE, A. M. 1952 *Q. J. Mech. Appl. Maths* **5**, 395.
BIRKHOFF, G. & ZARANTONELLO, E. H. 1957 *Jets, Wakes and Cavities.* Academic.
BRODETSKY, S. 1923 *Proc. R. Soc. Lond.* A **102**, 542.
DIAS, F., KELLER, J. B. & VANDEN-BROECK, J.-M. 1988 *Phys. Fluids* **31**, 2071.
FORBES, L. K. 1981 *J. Engng Maths* **15**, 287.
FORBES, L. K. 1988 *J. Engng Maths* **22**, 3.
FORBES, L. K. & SCHWARTZ, L. W. 1982 *J. Fluid Mech.* **114**, 299.
HAVELOCK, T. H. 1919 *Proc. R. Soc. Lond.* A **95**, 38.
HUNTER, J. K. & VANDEN-BROECK, J.-M. 1983 *J. Fluid Mech.* **136**, 63.
KELLER, J. B. 1957 *J. Appl. Phys.* **28**, 859.
KELLER, J. B. & GEER, J. 1973 *J. Fluid Mech.* **59**, 417.
LAMB, H. 1945 *Hydrodynamics.* Dover.
VANDEN-BROECK, J.-M. 1984 *Phys. Fluids* **27**, 2604.
VANDEN-BROECK, J.-M. 1986 *Phys. Fluids* **29**, 3084.
VANDEN-BROECK, J.-M. 1987 *Phys. Fluids* **30**, 2315.
VANDEN-BROECK, J.-M. & KELLER, J. B. 1986 *Phys. Fluids* **29**, 3958.
VANDEN-BROECK, J.-M. & KELLER, J. B. 1987 *J. Fluid Mech.* **176**, 283.